

Mott-Hubbard quantum criticality in paramagnetic CMR pyrochlores

L. Craco¹, C. I. Ventura², A. N. Yaresko³, and E. Müller-Hartmann¹

¹ *Institut für Theoretische Physik, Universität zu Köln, Zùlpicher Straße 77, 50937 Köln, Germany*

² *Centro Atómico Bariloche, 8400 - Bariloche, Argentina and*

³ *Max-Planck-Institut für Physik Komplexer Systeme, Nöthnitzer Straße 38, 01187 Dresden, Germany*

(Dated: January 24, 2019)

We present a correlated *ab initio* description of the paramagnetic phase of $\text{Tl}_2\text{Mn}_2\text{O}_7$, employing a combined local density approximation (LDA) with multiorbital dynamical mean field theory (DMFT) treatment. We show that the insulating state observed in this colossal magnetoresistance (CMR) pyrochlore is determined by strong Mn intra- and inter-orbital local electron-electron interactions. Hybridization effects are reinforced by the correlation-induced spectral weight transfer. Our result coincides with optical conductivity measurements, whose low energy features are remarkably accounted for by our theory. Based on this agreement, we study the disorder-driven insulator-metal transition of doped compounds, showing the proximity of $\text{Tl}_2\text{Mn}_2\text{O}_7$ to quantum phase transitions, in agreement with recent measurements.

PACS numbers: 75.47.-m, 75.50.-y, 71.15.-m, 71.27.+a, 71.30.+h, 78

Among the manganese oxides exhibiting colossal magnetoresistance (CMR) [1], the family of pyrochlores represented by $\text{Tl}_2\text{Mn}_2\text{O}_7$, [2, 3, 4] and the related compounds prepared by substitution of its different components [3, 5, 6] stands out. Though presenting similar coupling between magnetic and transport properties as the CMR perovskite manganites like $\text{La}_{1-x}\text{A}_x\text{MnO}_3$ ($\text{A}=\text{Ca}, \text{Sr}, \text{Ba}$), in the last nine years experiments have established many differences of their electronic properties [2], lattice behavior [2, 4, 7], spin dynamics [8], etc. In particular, transport and magnetism in CMR pyrochlores seem to be primarily related to different electronic orbitals [4, 5] coupled by hybridization. Mechanisms like double exchange, involving the transfer of electrons between neighbor $\text{Mn}^{3+} - \text{Mn}^{4+}$ ions which favours ferromagnetic alignment of the Mn core spins [9], and effects like Jahn-Teller distortions [10] were early discarded for pyrochlore compounds. A series of alternative theoretical proposals were put forward and explored in connection with the experimental results [11, 12, 13]. The first microscopic model studied for $\text{Tl}_2\text{Mn}_2\text{O}_7$ was the intermediate valence model (IVM) [11], proposed to explore the suggestion [4] of the presence of a small effective internal doping of the type $\text{Tl}_{2-x}^{3+}\text{Tl}_x^{2+}\text{Mn}_{2-x}^{4+}\text{Mn}_x^{5+}\text{O}_7$ ($x \sim 0.005$). The presence of spin-dependent hybridization gaps (or pseudogaps), and the predicted temperature and magnetic field dependent changes of the electronic structure allowed description of the observed magnetotransport [11]. In particular, the predicted evolution towards a gapped paramagnetic state above T_c explained the drastic reduction of the number of carriers at T_c in Hall data [2, 4]. Recently, thermopower and optical conductivity were qualitatively described using the IVM [14]. Majumdar and Littlewood [12] explored the scenario of spin fluctuations around T_c in the presence of very low carrier densities, first suggested in Refs. 4, 5. Considering Hund and superexchange couplings [12], they explained CMR in terms of spin po-

larons. Later, a generic effective model for $\text{Tl}_2\text{Mn}_2\text{O}_7$ [13] was introduced to explore and compare various proposals [2, 4, 12, 15, 16]. Interestingly, its electronic structure was shown [13] to exhibit similar features to the IVM model [11], for appropriate parameters, and the experimental spin dynamics [8] is described [17] if ferromagnetic superexchange is assumed [16].

$\text{Tl}_2\text{Mn}_2\text{O}_7$ is cubic at room temperature, with an fcc ($Fd\bar{3}m$) arrangement of corner-sharing Mn-O6 octahedra [2, 4]. Its large magnetoresistance accompanies a ferromagnetic metal to paramagnetic insulator transition, with T_c around 130 K [2, 3, 4]. The magnetization below T_c is believed to be determined by ferromagnetic superexchange coupling in the Mn^{4+} sublattice [4, 16]. Hall data indicate a very small electron-like carrier density [2] ($\sim 0.001-0.005 e/f.u.$), connected with the presence of extended Tl-6s orbitals hybridizing with O-2p and Mn- t_{2g} states near the Fermi level [15, 18, 19]. Upon Bi-substitution on the Tl site, magnetoresistance increases drastically and transport above T_c is strongly modified [6]. Notably, CMR is achieved at room temperatures, indicating the possibility of technological applications of $\text{Tl}_{2-x}\text{Bi}_x\text{Mn}_2\text{O}_7$ and related compounds.

The electronic band structure of $\text{Tl}_2\text{Mn}_2\text{O}_7$ has been calculated in local density approximation (LDA) by various groups [15, 18, 19]. They obtained similar results for the ferromagnetic metallic ground state, characterizing it as a half-metal with minority-spin free-electron-like carriers. However, no attention has been paid to the paramagnetic (PM) phase. In this work, we are presenting the first *ab initio* study of the paramagnetic phase of $\text{Tl}_2\text{Mn}_2\text{O}_7$. We found that LDA calculations predict a metallic paramagnetic state, in contrast to recent optical conductivity [20] and photoemission [21] experiments clarifying its insulating nature. By including multiorbital correlations through a combination of LDA with dynamical field theory (DMFT), we characterize the paramagnetic phase as a Mott-Hubbard insulator, with a

correlation-induced gap. We calculated optical conductivity contributions, and discuss our results in the context of recent experiments [20, 21] and effective model calculations [11]. Finally, we focus on the insulator-metal transition induced by chemical substitution.

LDA band structure calculations were performed for the experimental crystal structure of $\text{Tl}_2\text{Mn}_2\text{O}_7$ [19] using the LMTO method [22] in the atomic sphere approximation. The overlap of atomic spheres was decreased by adding two sets of empty spheres in $8a$ and $32e$ Wyckoff positions of the $Fd\bar{3}m$ space group. Our ferromagnetic phase results (not shown) agree with previous ones [15, 18, 19], while the electronic structure obtained for the paramagnetic phase is shown in Fig. 1. The differentiated hybridization between Tl and Mn with the two kinds of O atoms present is evident. Clearly, a metallic paramagnetic state is predicted by LDA, in contradiction with the insulating behavior recently established experimentally [20, 21].

Let us briefly outline the scheme of electronic structure calculation used. To include the real band structure and reliably treat the effect of correlations in the PM phase, as well as study metal-insulator transitions, we adopted the combined LDA+DMFT approach, which is becoming widely recognized as suitable for the realistic description of transition metal oxides. Previous similar applications of the technique include, e.g., the study of the insulator-metal transition in V_2O_3 and the ferromagnetic metallic state of CrO_2 [23]. The multi-orbital many-body Hamiltonian considered for the LDA+DMFT study of $\text{Tl}_2\text{Mn}_2\text{O}_7$ is:

$$H = \sum_{\mathbf{k}\alpha\beta\sigma} (\epsilon_{\mathbf{k}\alpha} + \epsilon_{\alpha}^0 \delta_{\alpha\beta}) c_{\mathbf{k}\alpha\sigma}^{\dagger} c_{\mathbf{k}\beta\sigma} + U \sum_{i\alpha} n_{i\alpha\uparrow} n_{i\alpha\downarrow} + U' \sum_{i\alpha\neq\beta} n_{i\alpha} n_{i\beta} - J_H \sum_{i\alpha\neq\beta} \mathbf{S}_{i\alpha} \cdot \mathbf{S}_{i\beta}, \quad (1)$$

where α, β denote the three t_{2g} orbitals. Due to the pyrochlore crystal field, the t_{2g} sub-shell is split into an a_{1g} singlet and an e'_g doublet. The size of the splitting $\Delta = \delta_{e'_g} - \delta_{a_{1g}}$ (δ_{α} being the center of gravity (c.g.) of the α band) within LDA is: $\Delta_{LDA} = 0.037$ eV. To avoid double-counting of interactions included already in the LDA in average, ϵ_{α}^0 reads; $\epsilon_{\alpha}^0 = \epsilon_{\alpha} - U(n_{\alpha\bar{\sigma}} - \frac{1}{2}) + \frac{J_H}{2}\sigma(n_{\alpha\sigma} - 1)$, with ϵ_{α} being the on-site energies of the t_{2g} orbitals. The first term in Eq. (1) describes the one-electron part of the Hamiltonian, including details of the pyrochlore crystal structure of $\text{Tl}_2\text{Mn}_2\text{O}_7$ through the LDA bandstructure: $\epsilon_{\mathbf{k}\alpha}$. The next three terms account for local correlation effects in the t_{2g} orbitals. Notice that we are keeping only the t_{2g} orbitals since, from LDA, the density of states (DOS) for the e_g bands is small near the Fermi level $E_F (\equiv 0)$, the $O - 2p$ bands lie approximately 1.5 eV below E_F and the $\text{Tl-}6s$ band about 2.5 eV above E_F . U (U') denotes the t_{2g} intra-

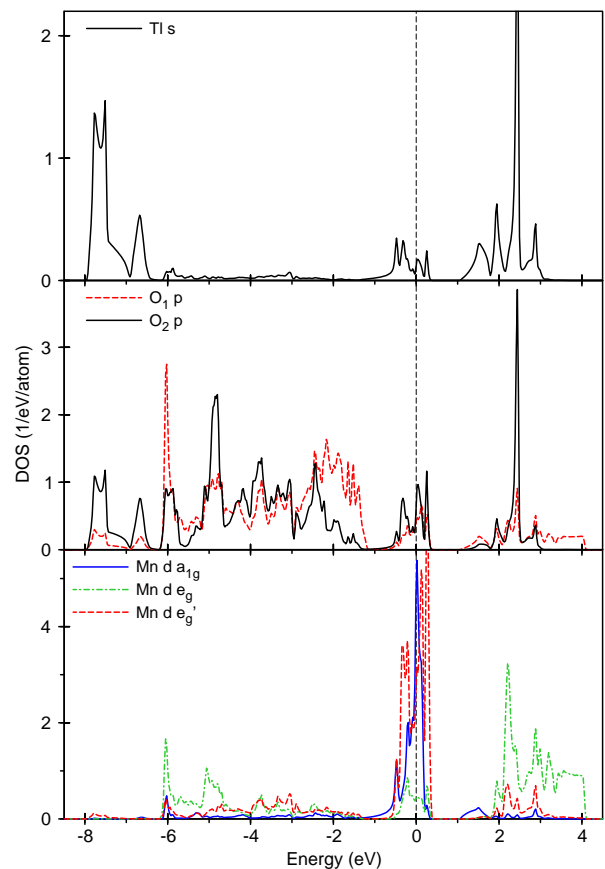


FIG. 1: (Color online) LDA band structure for paramagnetic $\text{Tl}_2\text{Mn}_2\text{O}_7$. O_1 (O_2) denotes Oxygen ions nearest to Mn (Tl).

(inter-) orbital local Coulomb interaction. The last term in Eq. (1) describes the Hund's rule coupling: being J_H poorly screened, we take it of the order of its atomic value in Mn^{4+} , $J_H = 1$ eV. Rotational invariance fixes: $U' = U - 2J_H$ [24].

We solve Eq. (1) in $d = \infty$ using multi-orbital iterated perturbation theory (MO-IPT) [23]. Assuming no symmetry breaking in the spin/orbital sector, we have $G_{\alpha\beta\sigma\sigma'}(\omega) = \delta_{\alpha\beta}\delta_{\sigma\sigma'}G_{\alpha\sigma}(\omega)$ and $\Sigma_{\alpha\beta\sigma\sigma'}(\omega) = \delta_{\alpha\beta}\delta_{\sigma\sigma'}\Sigma_{\alpha\sigma}(\omega)$. The DMFT solution involves (i) replacing the lattice model by a self-consistently embedded multi-orbital, asymmetric Anderson impurity model, and, (ii) a selfconsistency condition requiring the local impurity Green's function (GF) to be equal to the local GF for the lattice. The calculation follows the philosophy of the one-orbital IPT, with the Green functions and self-energies being matrices in the orbital indices. The equations for the multi-orbital case are the same as used before [23]. They are solved selfconsistently with the LDA density of states as input, until convergence is achieved.

We now present our LDA+DMFT results. In Fig. 2 we plot the t_{2g} density of states of the Mn-ions. Using $U = 7$ eV and $U' = 5$ eV as intra- and interorbital corre-

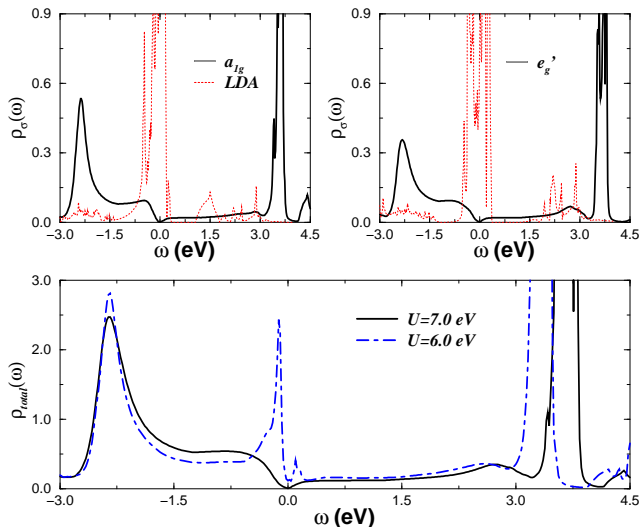


FIG. 2: (Color Online) LDA+DMFT (paramagnetic $\text{Tl}_2\text{Mn}_2\text{O}_7$): orbital-resolved (upper panels) and total (lower panel) Mn densities of states, for $U = 6, 7$ eV, $J_H = 1$ eV.

lation values, we obtain a clear Mott-Hubbard insulating state with an energy gap at the Fermi level. Compared to the LDA results of Fig. 1, spectral weight has been transferred to the Hubbard satellites close to maxima of the Tl and O bands, therefore reinforcing hybridization effects. Thus, one may envisage an overall gapped (insulating) state resulting from rehybridization, in a scenario with common features to those predicted by the effective IVM for paramagnetic $\text{Tl}_2\text{Mn}_2\text{O}_7$ [11]. Recent photoemission experiments at room temperature [21] confirmed the insulating nature of the paramagnetic phase. Finding a higher weight for O-2p at the upper edge of the valence band, in Ref. [21] $\text{Tl}_2\text{Mn}_2\text{O}_7$ is characterized as a charge-transfer insulator. Strong hybridization of O-2p and Mn- t_{2g} in the valence band is reported, and a 2-3 eV difference between the centers of gravity of the respective bands is estimated: the Mn one lying mainly at binding energies above 3 eV [21]. Interestingly, the correlation-induced shift of Mn spectral weight we find with respect to the LDA, goes in the same direction: shifting the Mn valence band to higher binding energies. Furthermore, Ref. 21 characterizes $\text{Tl}_2\text{Mn}_2\text{O}_7$ as close to a metal-insulator transition, in agreement with our results presented in Fig. 2.

We have employed our LDA+DMFT result for $U = 7$ eV to evaluate the t_{2g} contribution to the optical conductivity in the paramagnetic phase. Here, we consider only the t_{2g} intraband optical transitions: due to orthogonality of these orbitals, one would expect negligible contributions from interband transitions [25]. Within the t_{2g} -subshell the contributions to optical conductivity are calculated from:

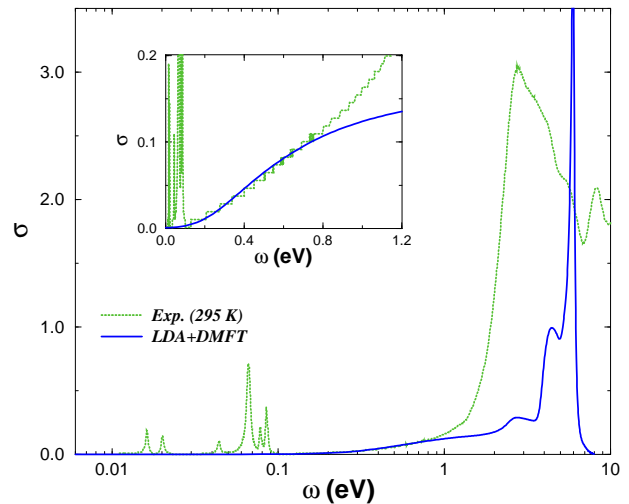


FIG. 3: (Color Online) Paramagnetic $\text{Tl}_2\text{Mn}_2\text{O}_7$: t_{2g} optical conductivity calculated with LDA+DMFT ($U=7$ eV), compared with expts. at $T=295$ K [20] Inset: Low-energy conductivity: LDA+DMFT vs. experiment at $T=295$ K.

$$\sigma(\omega) \propto \sum_{\alpha\mathbf{k}} \int d\omega' A_{\alpha\mathbf{k}}(\omega') A_{\alpha\mathbf{k}}(\omega' + \omega) \frac{f(\omega') - f(\omega' + \omega)}{\omega}$$

where $f(\omega)$ is the Fermi function and $A_{\alpha}(\mathbf{k}, \omega) = \frac{1}{\pi} \text{Im}[\omega - \Sigma_{\alpha}(\omega) - \epsilon_{\alpha\mathbf{k}}]^{-1}$ is the spectral density.

In Fig. 3 we show the calculated optical conductivity together with the experimental data at room temperature [20]. Apart from phonon related peaks (not included in our theory), a remarkable agreement is found at low energies (below 0.8 eV). The absence of optical response observed at very low energies evidences the insulating nature of the paramagnetic phase. For higher energies, a quantitative description of experiments would require to include the effect of inter-band charge-transfer excitations, from O-2p to Mn-3d bands, out of the scope of the present work.

Motivated by the remarkable agreement between our theory and the optical spectra, we now address the effect of disorder induced by chemical substitution [6]. The problem is treated within the LDA+DMFT(IPT+CPA) [26] approach, which treats disorder exactly in high-dimensions and has been used to describe the doping-driven insulator-metal transition in LaTiO_3 . However, differently from Ref. 26, here we consider only the effect of substitutional disorder: without the introduction of extra holes or electrons in the system. [Notice that in a binary-alloy distribution for disorder (CPA), a fraction x of the sites have an additional local potential v for an electron (or hole) hopping onto that site.] By this, we aim to account for a host of experimental realizations in the limit of small impurity con-

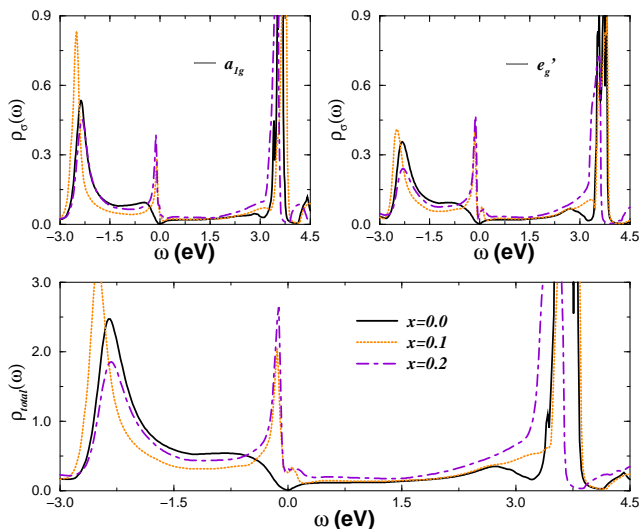


FIG. 4: (Color Online) Effect of disorder: orbital resolved (upper panels) and total (lower panel) DOS for $\text{Tl}_{2-x}\text{Bi}_x\text{Mn}_2\text{O}_7$. $U = 7$ eV, $U' = 5$ eV and $v = 2.5$ eV.

centrations [28]. Having in mind the possibility of technological applications upon *Bi*-substitution [6], in our calculation we use a disorder potential $v = 2.5$ eV, corresponding to the energy difference between the Tl-6s band and the Bi-6p band [27]. Fig. 4 shows that introduction of a small amount of impurities metallizes the system, in agreement with [6, 28]. Due to the pyrochlore structure, the Mott-Hubbard insulating state seems to be very unstable, allowing for first-order insulator-metal transitions upon small perturbations. According to our results, disorder or chemical pressure may drive $\text{Tl}_2\text{Mn}_2\text{O}_7$ into a bad metal fixed point, similar to that obtained for $U = 6$ eV (Fig. 2).

To conclude, we have presented the first *ab initio* study of the paramagnetic phase of $\text{Tl}_2\text{Mn}_2\text{O}_7$. Through the inclusion of local multiorbital Coulomb interactions and using a combined LDA+DMFT approach, we describe the insulating nature of this phase. Hybridization effects are reinforced by the spectral weight transfer due to strong correlations. The electronic structure obtained with $U = 7$ eV allows us to provide not only a consistent description of the low-energy optical conductivity data, but also a strong support for our picture of disorder effects induced by chemical substitution. In agreement with chemical doping studies and recent photoemission findings, our results indicate that $\text{Tl}_2\text{Mn}_2\text{O}_7$ is very near to quantum phase instabilities, and illustrate the interplay of strong multi-orbital correlations with disorder and pyrochlore structure effects, thus calling for investigation with higher resolution spectroscopies, including inverse photoemission.

We benefited from discussions with D.I. Khomskii and M.S. Laad. C.I.V. thanks B. Alascio, J.A. Alonso, M.

Foglio, M.N. Regueiro and G. Zampieri for comments and references. LC was supported by the SFB 608 of the Deutsche Forschungsgemeinschaft. C.I.V. is Investigador Científico of CONICET (Argentina), and thanks CONICET/DAAD for financial support as well as the Inst. für Theor. Physik, Univ. zu Köln, for hospitality.

-
- [1] H. Kuwahara and Y. Tokura, in *Colossal magnetoresistance, charge ordering and related properties of manganese oxides*, ed. by C. N. R. Rao and B. Raveau (World Scientific, Singapore, 1998).
 - [2] Y. Shimakawa, Y. Kubo, and T. Manako, *Nature* **379**, 55(1996).
 - [3] S. W. Cheong *et al.*, *Solid State Commun.* **98**, 163 (1996).
 - [4] M. A. Subramanian *et al.*, *Science* **273**, 81 (1996).
 - [5] A. P. Ramirez and M. A. Subramanian, *Science* **277**, 546 (1997).
 - [6] J. A. Alonso *et al.*, M. T. Fernández-Díaz, *Phys. Rev. Lett.* **82**, 189 (1999).
 - [7] Y. Shimakawa *et al.* *Phys. Rev. B* **55**, 6399 (1997); see also G. H. Kwei *et al.*, *Phys. Rev. B* **55**, R688 (1997).
 - [8] J. W. Lynn, L. Vasiliu-Doloc and M. A. Subramanian, *Phys. Rev. Lett.* **80**, 4582(1998).
 - [9] C. Zener, *Phys. Rev.* **82**, 403 (1951); P. W. Anderson and H. Hasegawa, *ibid.* **100**, 675 (1955); P. G. de Gennes, *ibid.* **181**, 141 (1960).
 - [10] A. J. Millis, P. B. Littlewood and B. I. Shraiman, *Phys. Rev. Lett.* **74**, 5144 (1995); A. J. Millis, B. I. Shraiman, and R. Mueller, *ibid.* **77**, 175 (1996).
 - [11] C. I. Ventura and B. Alascio, *Phys. Rev. B* **56**, 14533 (1997).
 - [12] P. Majumdar and P. B. Littlewood, *Phys. Rev. Lett.* **81**, 1314 (1998).
 - [13] C. I. Ventura and M. A. Gusmão, *Phys. Rev. B* **65**, 14422 (2002).
 - [14] M. E. Foglio and G. E. Barberis, *J. Mag. Mag. Mats.* **272-276**, 280 (2004); *Physica B* **354**, 35 (2004); *Phys. Rev. B* accepted preprint (2005).
 - [15] S. K. Mishra and S. Satpathy, *Phys. Rev. B* **58**, 7585 (1998).
 - [16] M. D. Núñez-Regueiro and C. Lacroix, *Phys. Rev. B* **63**, 14417 (2001).
 - [17] C. I. Ventura and M. Acquarone, *Phys. Rev. B* **70**, 184409 (2004).
 - [18] D. J. Singh, *Phys. Rev. B* **55**, 313 (1997).
 - [19] Y. Shimakawa *et al.*, *Phys. Rev. B* **59**, 1249 (1999).
 - [20] H. Okamura *et al.*, *Phys. Rev. B* **64**, 180409 (2001).
 - [21] J. Sánchez- Benítez *et al.*, *Applied Phys. Lett.* **84**, 4209 (2004).
 - [22] O. K. Andersen, *Phys. Rev. B* **12**, 3060 (1975).
 - [23] L. Craco, M. S. Laad and E. Müller Hartmann, *Phys. Rev. Lett.* **90**, 237203 (2003); M. S. Laad, L. Craco and E. Müller Hartmann, *Phys. Rev. Lett.* **91**, 156402 (2003).
 - [24] K. Held and D. Vollhardt, *Eur. Phys. J. B* **5**, 473 (1998).
 - [25] E. Pavarini *et al.*, cond-mat/0504034.
 - [26] L. Craco *et al.*, *Phys. Rev. B* **70**, 195116 (2004).
 - [27] J. Park *et al.*, *Phys. Rev. B* **69**, 165120 (2004).
 - [28] P. Velasco *et al.*, *J. Mag. Mag. Mats.* **242**, 725 (2002); P. Velasco *et al.*, *Phys. Rev. B* **67**, 104403 (2003).